Journal of Hazardous Materials 392 (2020) 122276

Contents lists available at ScienceDirect

Journal of Hazardous Materials

journal homepage: www.elsevier.com/locate/jhazmat

Levels, sources, isotope signatures, and health risks of mercury in street dust across China

Guangyi Sun[a,b], Xinbin Feng[a,*], Chenmeng Yang[a,b], Leiming Zhang[c], Runsheng Yin[d], Zhonggen Li[e,*], Xiangyang Bi[f], Yunjie Wu[f,a]

[a] State Key Laboratory of Environmental Geochemistry, Institute of Geochemistry, Chinese Academy of Sciences, Guiyang, 550081, China
[b] University of Chinese Academy of Sciences, Beijing, 100049, China
[c] Air Quality Research Division, Science and Technology Branch, Environment and Climate Change Canada, Toronto, M3H5T4, Canada
[d] State Key Laboratory of Ore Deposit Geochemistry, Institute of Geochemistry, Chinese Academy of Sciences, Guiyang, 550081, China
[e] College of Resources and Environment, Zunyi Normal University, Zunyi, 563006, China
[f] School of Earth Sciences, China University of Geosciences, Wuhan, 430074, China

GRAPHICAL ABSTRACT

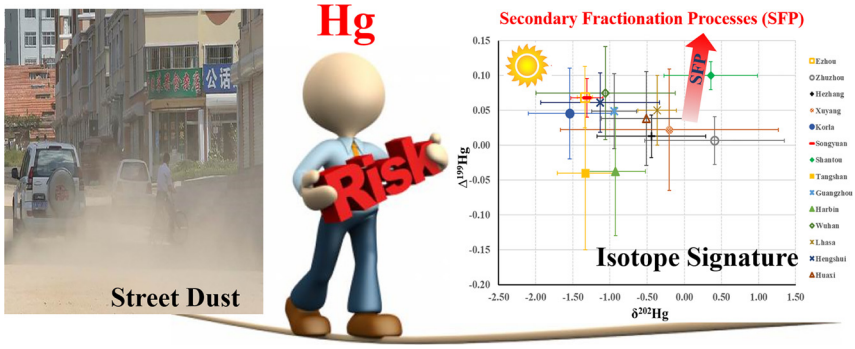

ARTICLE INFO

Editor: Deyi Hou

Keywords:
Urban environment
Mercury source
Street dust
Health risk
Assessment

ABSTRACT

Spatial distribution and isotope signature of mercury (Hg) in street dusts across China were investigated by collecting dust samples from 14 cities and reviewing previously published data from an additional 46 cities. Potential sources of street dust and the associated health risks to humans were also assessed. The total Hg (THg) concentrations in street dust ranged from 0.020–39.1 mg kg^{-1} with an average of 0.433 ± 0.185 mg kg^{-1} in the 60 cities. Street dust samples collected from 14 cities were characterized by slightly negative δ^{202}Hg (−0.61 ± 0.92‰) and near-zero Δ^{199}Hg (−0.03 ± 0.08‰) values, and coal combustion and industrial activities were estimated to be the major sources of Hg in street dust. The estimated average probable daily intake (PDI) of THg from street dust exposure for adults and children (1.36E–03 and 1.27E–02 μg d^{-1} kg^{-1}, respectively) were comparable to their respective exposures via rice consumption in China. Children being exposed to THg in dust is a major concern in mercury mining areas (e.g., Wangshan and Xunyang), and may also be a concern in cities with major coal-based industries and nonferrous metal smelting. Results from this study suggest that exposure to street dust is not a primary MeHg exposure pathway in China.

* Corresponding authors.
E-mail addresses: fengxinbin@vip.skleg.cn (X. Feng), lizhonggencn@126.com (Z. Li).

https://doi.org/10.1016/j.jhazmat.2020.122276
Received 29 October 2019; Received in revised form 26 January 2020; Accepted 10 February 2020
Available online 11 February 2020
0304-3894/

1. Introduction

Atmospheric dustfall refers to particles that fall naturally to the ground under the influence of gravity and normal environmental conditions and is the general term for solid particles with particle sizes mostly larger than 10 μm (Du et al., 2004). Particles smaller than 10 μm can also settle to the ground through dry deposition process (Sun et al., 2019a, 2019b). Dust particles are non-uniform mixtures of inorganic non-metallic and metallic particles, and organic particles. Among these, heavy metals are hazardous materials that are loosely bound to the surface of dust particles (Marx et al., 2008; Li et al., 2013; Dehghani et al., 2018; Nabizadeh et al., 2018; Dehghani et al., 2019).

In addition to natural sources (e.g., local soil, geologic origin, and parent materials), human activities also produce dust particles. For example, large amounts of toxic and harmful substances are released from motor vehicle emissions, tire friction, and industrial and construction activities, which can accumulate onto street dust through various physical and chemical processes (Marcazzan et al., 2001). Toxic and harmful substances (such as heavy metals and polycyclic aromatic hydrocarbons) have caused widespread concern in the context of human and ecosystem health (Wright et al., 2018). Toxic substances in urban dust can enter the human body directly through breathing, swallowing, and absorption into the skin, posing direct hazards to the human body, and in particular to children (Qasemi et al., 2019; Zhang et al., 2014a, 2014b, 2014c, 2014d).

Mercury (Hg) is one of the toxic heavy metals that needs to be monitored in various environmental media including street dust. Previous studies of street dust in China have focused more on other heavy metals (e.g., Pb, Cd, Cu, and Zn) than Hg, and the few studies of Hg were focused on individual cites or small regions (Hou et al., 2019; Yang et al., 2019; Wei and Yang, 2010; Streets et al., 2005). A survey of Hg contents in street dust on a national scale is urgently needed, especially considering the recent high levels of air pollution across China. Furthermore, China is currently considered to be the largest global Hg emitter (Fu et al., 2012) due to its rapid economic development. It was shown that 42.2 % of mercury emitted from coal combustion processes, 19.5 % from nonferrous metal smelting processes, 34.5 % from cement clinker production, and 3.8 % from waste incineration processes settled in urban areas (Wu et al., 2018). In addition, waste incineration is currently an important pollution source in urban environments, and 34 % of the Hg in municipal solid waste is discharged into the atmosphere from the exhaust stack while 65 % is retained in the fly ash (Duan et al., 2016).

Unlike Cu, Zn, Cd and Pb in street dust, which have been paid more attention globally and studied extensively in recent years (Wang et al., 2016; Hou et al., 2019), few data are available for the amount of Hg present in street dust (Sun et al., 2013; Brown et al., 2019; Lin et al., 2019). In addition, concentrations, source identification, spatial distribution characteristics and health risk assessments of Hg contamination on a national scale are limited. Thus, a comprehensive survey of Hg in street dust across China is urgently needed. Previous studies regarding Hg contamination associated with source analyses of street dust mostly used principal component analysis, factor analysis, and positive matrix factorization (Sun et al., 2013; Men et al., 2018), while no studies have yet used Hg isotopes, which may provide direct evidence for determining Hg sources, as well as insight into the geochemical processes that have occurred.

Mercury isotope compositions have been measured in different environmental media, such as ore, coal, soil/sediments, and atmospheric and biological samples (Yin et al., 2014; Sun et al., 2016a; Blum and Johnson, 2017). The large differences in Hg isotope compositions between the different media allow for their use as a powerful tool for identifying potential Hg sources and geochemical processes (Sun et al., 2016a; Wiederhold, 2010; Demers et al., 2015). Such isotope techniques were used in this study to measure Hg isotope compositions in street dust samples from 14 cities in China, the data from which they are used to explore Hg pollution sources. Understanding Hg sources in urban environments and the corresponding geochemical processes are of particular interest for assessing Hg impacts on human health and for proposing Hg emission control policies.

2. Materials and methods

2.1. Sample collection

To ensure a good representation of sampling locations, dust samples were collected from 14 Chinese cities using the approximate grid distribution method (3 km × 3 km resolution in each city). The cities was chosen based on spatial distribution and industrial types present in the cities. The 14 cities were Ezhou (EZ), Guangzhou (GZ), Harbin (HRB), Hengshui (HS), the District of Huaxi in Guiyang (HX), Hezhang (HZ), Lhasa (LS), Shantou (SHT), Songyuan (SY), Tangshang (TS), Wuhan (WH), Korla (KRL), Xunyang (XY), and Zhuzhou (ZZ). The distribution and accumulation of surface dust is generally restored to normal levels in 48 h after a rainfall (Sun et al., 2013). The dust samples in this study were therefore collected on calm and clear days 72 h after a rainfall. Three dust samples (approximately 100 g each) were collected from a central street in every grid using a plastic dustpan and a brush and were then mixed together and sealed in a plastic bag. A total of approximately 420 mixed dust samples (each weighting ~300 g) were collected from the 14 cities listed previously. These samples were first air-dried, and any debris were removed using stainless steel tweezers. The samples were then ground into small pieces using an agate mortar and pestle and passed through a 200 mesh nylon sieve.

To obtain a complete understanding of domestic street dust pollution across China, previously published data on street dust mercury contents were reviewed and combined with the data collected in this study (Table 1). The previously published data were obtained from 46 Chinese cities including Guiyang (GY), Xi'an (XA), Chongqing (CQ), Beijing (BJ), Huainan (HN), Shanghai (SH), Wuhu (WHU), Changchun (CC), Wuda (WD), Changji (CJ), Baotou (BT), Kaifeng (KF), Suzhou (SZ), Wen'an (WA), the Ebinur Basin (EBB), Changsha (CS), Nanjing (NJ), Taipei (TP), Jining (JN), Huludao (HLD), Baoji (BJ), Hohhot (HHT), Urumqi (UQ), Shijiazhuang (SJZ), Taiyuan (TY), the Songnen Plain (SNP), Changzhou (CZ), Nantong (NT), Taichang (TC), Jiangdu (JD), Rugao (RG), Yixing (YX), Tongling (TL), Shunde (SD), Jiangyou (JY), Qingdao (QD), Ningbo (NB), Gannan (GN), Chengdu (CD), Haidong (HD), Linyi (LY), the Taiyuan Basin (TYB), Yuanping (YP), the East Junggar Basin (EJB), Changji (CJ), Wanshang (WS), and Hongkong (HK). Sampling sites in each city covered different functional areas (i.e., residential, commercial, industrial, cultural, and educational areas) (Tian et al., 2006; Dai, 2016; Men et al., 2018; Yao et al., 2017a, 2017b; Chen and Luan, 2010; Fang et al., 2009; Yang, 2008; Hou et al., 2015; Han et al., 2017; Duan et al., 2016; Ma et al., 2016; Abuduwailil et al., 2015; Li et al., 2014, 2015a, 2015b; Li and Liao, 2018; Zhang et al., 2014a, 2014b, 2014c, 2014d; Dai et al., 2014; Li et al., 2013; Sun et al., 2013; Huang et al., 2012). The cities involved in this study and the distribution of Hg in street dust in Chinese cities are shown in Fig. 1. Mercury levels for each city are represented by arithmetic averages.

2.2. Sample analytical procedure

The total Hg (THg) concentrations of all the street dust samples were analyzed using thermal decomposition and Zeeman atomic absorption spectrometry (Lu et al., 2019) with an RA915+ Hg analyzer coupled with a PYRO-915+ attachment (Lumex-Marketing Jsc, Russia). The quality control for this procedure consisted of method blanks, certified reference materials (CRMs), and duplicates. The average THg concentrations of two CRMs, BCR-482 and GSS-4, were 473 ± 10 and 598 ± 35 μg kg^{-1} (2SD, n = 10), which are comparable to their certified values of 480 ± 20 and 590 ± 50 μg kg^{-1}, respectively, and the duplicate sample bias was less than 10 %.

Table 1
Summary of total mercury concentration of street dust in Chinese cities.

Locations	Province	THg (mg kg^{-1})			Urban regional Characteristics	Reference
		min	max	average		
Huainan (HN)	Anhui	0.03	3.02	0.197	Coal-based industries	Tang et al., 2017
Wuhu (WHU)	Anhui	0.011	1.477	0.23		Fang et al., 2009
Tongling (TL)	Anhui	0.102	1.44	0.51		Li et al., 2015a, 2015b
Beijing center (BJC)	Beijing	0.04	3.69	0.33		Yu et al., 2016a, 2016b
Miyun Town (MYT)	Beijing	0.07	6.16	0.81		Yu et al., 2016a, 2016b
Miyun County (MYC)	Beijing	0.02	0.63	0.08		Yu et al., 2016a, 2016b
Beijing (BJ)	Beijing	0.04	0.78	0.16		Men et al., 2018
Chongqing (CQ)	Chongqing	0.02	0.71	0.16		Dai et al., 2015
Guangzhou (GZ)	Guangdong		0.48	0.235		Huang et al., 2012 and this study
Shantou (SHT)	Guangdong	0.06	12.59	3.42	E-waste Dismantling Area	this study
Shunde (SD)	Guangdong	0.05	2.517	0.92		Li et al., 2015b
Guiyang (GY)	Guizhou	0.097	2.58	0.379		Dai, 2016
Hezhang (HZ)	Guizhou	0.08	0.89	0.22	Lead and zinc smelting	this study
Wanshan (WS)	Guizhou	1	39.12	30.59	Mercury's capital	Lin, 2017 and this study
Tangshan (TS)	Hebei	0.06	1.57	0.2669		Chen and luan, 2011 and this study
Wen'an (WA)	Hebei	0.02	0.9	0.15		Li et al., 2015b
Shijiazhuang (SJZ)	Hebei	0.15	0.775	0.36		Gu, 2014
Hengshui (HS)	Hebei	0.029	10.687	0.349		this study
Harbin (HRB)	Heilongjiang	0.09	1.047	0.25		Gu, 2014 and this study
Songnen plain (SNP)	Heilongjiang	0.01	0.62	0.12		Gu, 2014
Gannan (GN)	Heilongjiang	0.015	0.219	0.13	Farming	Deng et al., 2012
Kaifeng (KF)	Henan	0.1	3.6	0.5	Tourist industry	Duan et al., 2016
HongKong (HK)	HongKong			0.6		Huang et al., 2012
Wuhan (WH)	Hubei	0.15	10.59	1.66		Sun et al., 2013 and this study
Ezhou (EZ)	Hubei	0.044	0.089	0.067		this study
Changsha (CS)	Hunan	0.09	0.23	0.15		Li et al., 2015a
Zhuzhou (ZZ)	Hunan	0.08	14.6	0.92	Equipment manufacturing /non-ferrous metal smelting	Li et al., 2013 and this study
Wuda (WD)	Inner Mongolia	0.003	6.453	0.293	Coal mining area (coal fire)	Li et al., 2017
Baotou (BT)	Inner Mongolia	0.0239	0.192	0.0649	Rare earth capital	Han et al., 2017
Huhhot (HHT)	Inner Mongolia	0.051	9.461	0.59	Power generation industry	Gu, 2014
Suzhou (SZ)	Jiangsu	0.03	2.18	0.18	Mining (Pb, Zn, Cu, Ag, and pyrite)	Ma et al., 2016
Nanjing (NJ)	Jiangsu	0.063	1.16	0.39	Center for science, education and culture	Li et al., 2014
Changzhou (CZ)	Jiangsu	0.32	0.53	0.41	Machine building industry	Liu et al., 2009
Nantong (NT)	Jiangsu	0.18	0.81	0.42		Liu et al., 2009
Taichang (TC)	Jiangsu	0.32	0.53	0.37		Liu et al., 2009
Jiangdu (JD)	Jiangsu	0.18	1.03	0.43		Liu et al., 2009
Rugao (RG)	Jiangsu	0.18	0.61	0.3		Liu et al., 2009
Yixing (YX)	Jiangsu	0.098	0.5	0.2		Liu et al., 2009
Changchun (CC)	Jilin	0.53	1.127	0.56	Automobile industry	Yang, 2008
Songyuan(SY)	Jilin	0.002	0.22	0.042		this study
Huludao (HLD)	Liaoning	0.119	5.212	1.22	Non-ferrous metal metallurgy	Gu, 2014
Haidong (HD)	Qinghai	0.076	0.315	0.129	Large cement plant	Yao et al., 2017a, 2017b
Linyi (LY)	Shandong	0.04	3.3	0.56	Trade logistics	Shao et al., 2019
Jining (JN)	Shandong	0.016	2.188	0.183	Tourist and light industry	Dai et al., 2014
Qingdao (QD)	Shandong	0.031	0.97	0.19		Zhang et al., 2014a
Wujing (WJ)	Shanghai	0.033	0.831	0.1383		Hou et al., 2015
Yangpu (YP)	Shanghai	0.1	1	0.5		Li et al., 2015b
Residential area (RA)	Shanghai		2.33	0.2		Zhang et al., 2015
Xi'an (XA)	Shaanxi	0.108	5.212	0.6		Gu, 2014
Baoji (BJ)	Shaanxi	0.5	2.3	1.1		Gu, 2014
Xunyang(XY)	Shaanxi	2.99	14.01	3.500		this study
Yuanping (YP)	Shanxi	0.04	2.78	0.43	Coal transportation hubs	Li and Liao, 2018
Taiyuan basin (TYB)	Shanxi	0.091	0.367	0.191	Coal base	Lai et al., 2008
Taiyuan (TY)	Shanxi	0.091	0.367	0.19	Coal mining area	Gu, 2014
Jiangyou (JY)	Sichuan	0.26	7.67	0.28		Li et al., 2015b
Chengdu (CD)	Sichuan	0.028	5.281	1.063		Tan et al., 2008
Taipei (TP)	Taiwan			1.59		Zhang et al., 2014a, 2014b, 2014c, 2014d
Lhasa (LS)	Tibet	0.032	1.346	0.305		this study
East Junggar Basin (EJB)	Xinjiang	0.02	5.18	0.19	Coal base	Yang et al., 2019
Changji (CJ)	Xinjiang	0.02	5.18	0.19		Li et al., 2015b
Ebinur Basin (EB)	Xinjiang	0.01	0.79	0.04		Abuduwailil et al., 2015
Urumqi (UQ)	Xinjiang	0.038	0.434	0.14		Gu, 2014
Korla (KRL)	Xinjiang	0.004	0.038	0.019		this study
Hangzhou (HZ)	Zhejiang	0.19	1.76	0.7		Huang et al., 2012
Ningbo (NB)	Zhejiang	0.091	0.323	0.249		Mao et al., 2016

Approximately 25 % of the dust samples collected were pre-concentrated into 5 mL of a 40 % mixed acid solution (v/v, $3HNO_3$/1HCl) using a double-stage combustion protocol for Hg isotope analysis as described earlier (Huang et al., 2015; Sun et al., 2016a, 2016b). The mercury isotope ratios were measured using cold vapor multi-collector inductively coupled plasma mass spectrometry (CV-MC-ICPMS, Nu II Instruments) at the State Key Laboratory of Environmental Geochemistry, Institute of Geochemistry, Chinese Academy of Sciences, following the method described by Yin et al. (2016a). The MC-ICPMS instrumental mass bias was corrected using standard-sample-standard

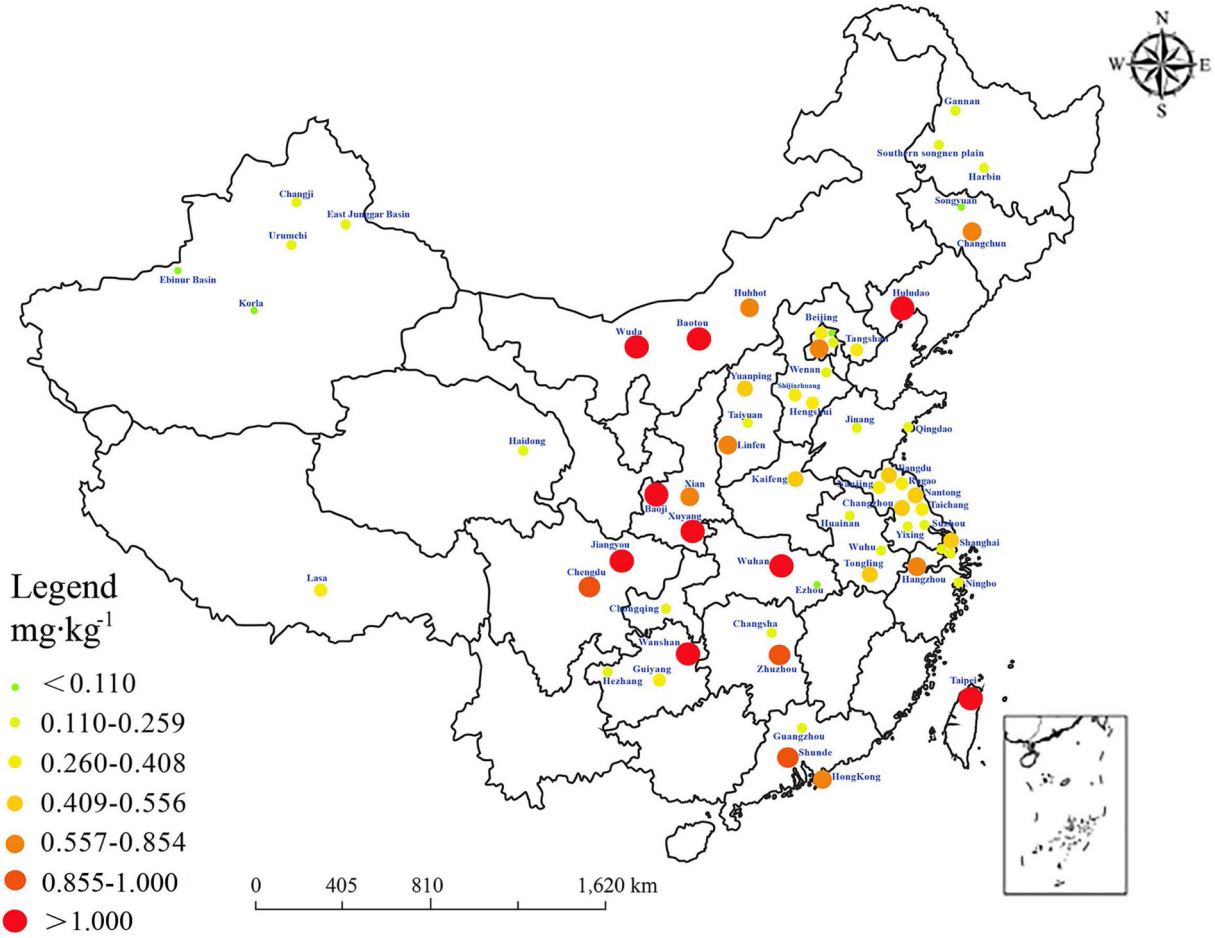

Fig. 1. Cities involved in this study and the distribution patterns of total Hg in street dust around China.

bracketing with NIST3133 Hg at matching concentrations. The Hg isotopic composition of the mass-dependent fractionation (MDF) is reported using delta notation (δ) in units of per mil, referenced to the bracketed NIST3133 Hg standard, which is obtained using the following equation (Blum and Bergquist, 2007):

$$\delta^{xxx}Hg = \left[\frac{(xxxHg/^{198}Hg)_{sample}}{(xxxHg/^{198}Hg)_{NIST3133}}\right] \times 1000 \quad (1)$$

where XXX represents 199, 200, 201, or 202.

The mass independent fraction (MIF) values are expressed using the "capital delta (Δ)" notation (‰), which is the difference between the measured values of δ^{199}Hg, δ^{200}Hg, and δ^{201}Hg, and those predicted for δ^{202}Hg using the kinetic MDF law:

$$\Delta^{199}Hg = \delta^{199}Hg_{observed} - \delta^{199}Hg_{predicted} = \delta^{199}Hg_{observed} - (\delta^{202}Hg \times 0.252) \quad (2)$$

$$\Delta^{200}Hg = \delta^{200}Hg_{observed} - \delta^{200}Hg_{predicted} = \delta^{200}Hg_{observed} - (\delta^{202}Hg \times 0.502) \quad (3)$$

$$\Delta^{201}Hg = \delta^{201}Hg_{observed} - \delta^{201}Hg_{predicted} = \delta^{201}Hg_{observed} - (\delta^{202}Hg \times 0.752) \quad (4)$$

The UM-Almaden standard (n = 10) was used to determine the analytical veracity of the isotopic analyses. The overall mean values of δ^{202}Hg, Δ^{199}Hg, Δ^{200}Hg, and Δ^{201}Hg for the UM-Almaden standards were −0.55 ± 0.07‰, −0.05 ± 0.04‰, −0.00 ± 0.02‰ and 0.04 ± 0.03‰ (2SD, n = 10), respectively, which agree with previously reported values (Bergquist and Blum, 2007). In addition, digest replicates of GSS-4 (n = 7) were analyzed and the isotopic ratios of δ^{202}Hg, Δ^{199}Hg, Δ^{200}Hg, and Δ^{201}Hg were −1.70 ± 0.15‰, −0.40 ± 0.08‰, −0.00 ± 0.04‰ and −0.30 ± 0.07‰ (2SD, n = 7), respectively, which are similar to published values (Estrade et al., 2010). Data uncertainties (± 2σ) reported here reflect the larger values of either the external precision of the replication of the standard solutions (UM-Almaden and GSS-4) or sample replicates.

2.3. Statistical analyses

All data were analyzed using the statistics software package SPSS 24.0 for Windows. Relationships between the measured variables were characterized by linear regressions. For all statistically significant relationships, the Hg concentrations and Hg isotope data for all samples were compared using ANOVA at a 5% significance level. The cumulative probabilities of Hg health risk exposure were analyzed using a Monte Carlo simulation (Hou et al., 2019) conducted in Crystal Ball (version 11.1.2), which was loaded in Microsoft Excel.

2.4. Human health risk assessment method

To estimate potential adverse health effects caused by the total Hg and MeHg exposure through direct ingestion of street dust, the probable daily intake (PDI) values for adults and children, proposed by the United States Environmental Protection Agency (USEPA, 1989; Rostami et al., 2019; Yunesian et al., 2019), were calculated. The probable daily intake (PDI) (μg kg^{-1} d^{-1}) equation shown below was used to calculate the exposure level of the general adult population in China:

$$PDI = (C \times IR \times EF \times ED)/(BW \times AT) \quad (5)$$

where C is the concentration of THg or MeHg in the dust (μg kg^{-1}), IR is

Table 2
Summary of parameters used in the risk assessment.

Parameters	Unit	Values	References
EF	d a^{-1}	365	USEPA, 1986
ED	a	30	USEPA, 1989
BW	kg	70 (Adult) 15 (Children)	USEPA, 1986, 1989
AT	d	365ED	USEPA, 1986
Average IR in China			
Dust	mg d^{-1}	100 (Adult) 200 (Children)	USEPA, 2001, 2011
RfDs			
THg	μg $kg^{-1}d^{-1}$	0.16	OEHHA, 2008
MeHg	μg $kg^{-1}d^{-1}$	0.1	USEPA, 2010

the ingestion rate (kg person^{-1} day^{-1}), *EF* is the exposure frequency, *ED* is the exposure duration, *BW* is the average body weight, and *AT* is the average exposure time.

The description and values of the factors used in Eq. (5) are outlined in Table 2.

3. Results and discussion

3.1. Mercury contents of dust samples

Mercury concentrations in the dust samples from the 60 cities ranged from 0.020–39.1 mg kg^{-1}, with an average of 0.433 ± 0.185 (1SD) mg kg^{-1} and a median value of 0.457 mg kg^{-1} shown in Fig. 1 and Table 1. A positive coefficient of skewness (0.94) indicates that the mercury concentrations do not follow a normal distribution pattern, and this was confirmed by Kolmogorov–Smirnov (K–S) normality tests ($p > 0.05$).The presence of some highly contaminated locations was revealed through our analyses. In addition, the average value of Hg in street dust samples was 7 times higher than that of the Chinese background value (0.065 mg kg^{-1}) (Wang, 2015; CEPA, 1990) and lower than the Chinese guideline for soils (GB 15618-1995 Class II, 1 mg kg^{-1}). However, 14.8 % of the samples exceeded the Chinese guideline for soils.

Fig. 1 and Table 1 clearly show that mercury pollution is more severe in southwestern and southeastern China than in northwestern and northeastern China. This may be related to industrial development in the western region of China in recent years, while the developed eastern regions have taken the lead on environmental governance. In addition, the results showed obvious characteristics of point source pollution. More specifically, Hg ore exploitation and smelting in Xunyang (in Shaanxi province) and Wanshan (in Guizhou province) produced the highest mercury pollution with mean values of 3.50 mg kg^{-1} and 30.59 mg kg^{-1}, respectively; and uncontrolled e-waste recycling in Shantou and a large steel plant in Wuhan also produced high mercury levels, with average values of 3.42 mg kg^{-1} and 1.66 mg kg^{-1}, respectively. In addition, coal-based industries and lead and zinc smelting also caused high Hg contents in dust samples, such as in Huhhot (range: 0.051–9.46 mg kg^{-1}, mean: 0.590 mg kg^{-1}), Wuda (range: 0.003–6.45 mg kg^{-1}, mean: 0.804 mg kg^{-1}), Zhuzhou (range: 0.08–14.6 mg kg^{-1}, mean: 0.920 mg kg^{-1}), and Huludao (range: 0.119–5.21 mg kg^{-1}, mean: 1.22 mg kg^{-1}). Mercury concentrations in the dust samples were closely related to local industry types and pollution control technology in use, and were unrelated to the level of economic development (i.e., the GDP).

From a global perspective, mercury concentrations in Chinese street dust samples are higher than those in Luanda, Angola (0.13 mg kg^{-1}; Lu et al., 2009), Kavala, Greece (0.1 mg kg^{-1}; Nazarpour et al., 2017), and Ottawa, Canada (0.02 mg kg^{-1}; Nazarpour et al., 2017), and lower than those in Avilés, Spain that mainly with the steel industry and Zn and Al metallurgy activities (2.56 mg kg^{-1}; Ordóñez et al., 2015), Bhilai, India that mainly with the steel industry activities (2.10 mg kg^{-1}; Ambade and Litrupa, 2012), and Ahvaz (2.53 mg kg^{-1}) and Shiraz (1.05 mg kg^{-1}) in Iran that with high traffic levels and intense industrial activities (Nazarpour et al., 2017).

3.2. Methylmercury contents in dust samples

Methylmercury (MeHg) concentrations in street dust have been previously reported from three cities in China, that had a range of 0.092–3.88 μg kg^{-1} from all samples, and mean concentrations of 0.55, 0.39, and 1.57 μg kg^{-1} for Xiamen, Guangzhou, and Wuhan, respectively (Liang et al., 2009; Huang et al., 2012; Sun et al., 2013). The corresponding MeHg/THg ratio ranged from 0.004 % to 1.63 %, with mean values of 0.28 %, 0.22 %, and 0.20 % for Xiamen, Guangzhou, and Wuhan, respectively (Liang et al., 2009; Huang et al., 2012; Sun et al., 2013). Previous studies on the health impacts of MeHg have mostly focused on fish and rice (Zhao et al., 2019; Zhang et al., 2010), and few have focused on MeHg in street dust, especially in developing countries with serious dust exposure potential, such as China and India.

3.3. Source identification

Mercury isotope ratios can provide some insights on Hg sources and atmospheric cycling processes. Since Hg in atmospheric aerosols is photoreduced by a certain degree after being emitted into the atmosphere (Huang et al., 2019; Xu et al., 2017), the slope of Δ^{199}Hg vs. Δ^{201}Hg in aerosol samples can provide some information regarding the extent of Hg photoreduction and oxidation (Xu et al., 2017; Sun et al., 2016a). In this study, the correlation of Δ^{199}Hg vs. Δ^{201}Hg was poor (Fig. S1, *slop* = 1.23, $r^2 = 0.35$, $p > 0.05$) compared to previously reported values of 1.6 for Br-initiated oxidation, 1.9 for Cl-initiated oxidation (Sun et al., 2016a), and 1 for Hg^{2+} reduction (Zheng and Hintelmann, 2010), indicating that mercury in dust samples may be affected by multiple processes. However, the poor correlation of Δ^{199}Hg vs. Δ^{201}Hg suggest that the isotopic signatures resulted primarily from the variations of emission sources, rather than from secondary fractionation processes (eg. photoreduction). Atmospheric dustfall generally refers to solid particles that fall to the ground quickly, and mostly have an aerodynamic diameter greater than 10 μm (Du et al., 2004). Thus, Hg in street dust should not be influenced by photoreduction in the atmosphere due to its short lifetime. At the same time, Huang et al. (2020) found that mercury isotopic compositions of TSP remain unchanged after dry deposition or resuspension.

The characteristics of mercury isotope ratios in the dust samples and potential source materials are shown in Fig. 2 and Table S1. δ^{202}Hg was in the range of −2.22 to 2.50‰ (or variations of 4.72‰) and Δ^{199}Hg in the range of −0.21 to 0.15‰ (or variations of 0.36‰). Normal distributions of these values were identified by using the Shapiro-Wilk test. Thus, the arithmetic mean and standard deviation were used to describe the data, which were characterized by slightly negative δ^{202}Hg values (−0.61 ± 0.92‰) and near-zero Δ^{199}Hg (−0.03 ± 0.08‰) values in the 14 cities sampled in this study. The broad variations in the Hg isotopic composition is clear evidence of mixed dust from both background and human activities (Fig. 2). No significant correlation (t-test, p = 0.929) was observed between δ^{202}Hg and Δ^{199}Hg in each individual city, implying that negative MDF and negative MIF did not occur simultaneously. δ^{202}Hg from the various cities increased in the order of KRL < ER < TS < SY < HS < WH < GZ < HRB < HX < HZ < LS < XY < 0 < SHT < ZZ, while Δ^{199}Hg increased in the order of TS < LS < SHT and 11 other cities that were all similar (Fig. 2), suggesting that different human activities in different cities accounted for the various mercury pollution sources (Huang et al., 2016; Das et al., 2016; Xu et al., 2017).

Previous studies on TSP isotopic composition were conducted in Beijing (Huang et al., 2020), Xiamen (Huang et al., 2018), Xi'an (Xu et al., 2017), Guiyang (Yu et al., 2016b), Dameishan Atmospheric Observatory (DAO) (Yu et al., 2016b), and semi-rural Grand Bay,

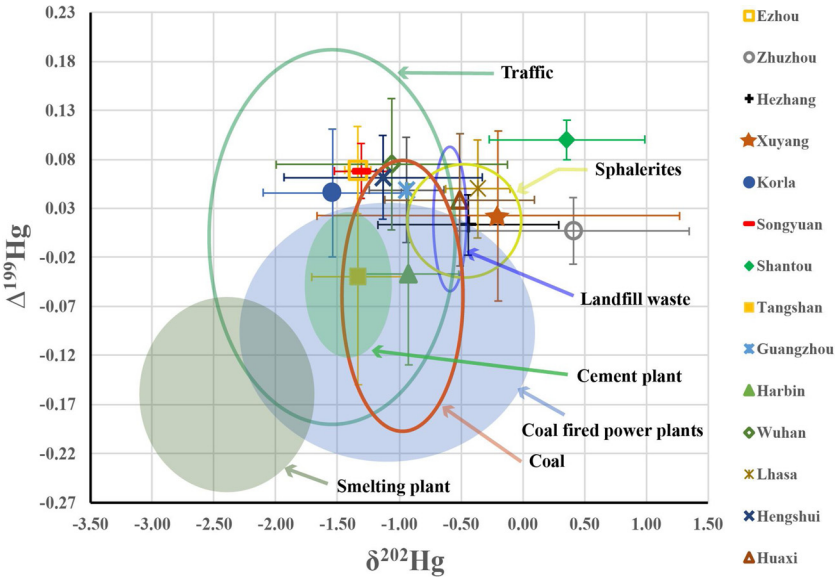

Fig. 2. Two-dimensional Hg isotope plot with mass-dependent fractionation (MDF, δ^{202}Hg) vs mass-independent fractionation (MIF, Δ^{199}Hg) in street dust samples and the potential pollution sources (Coal-fire power plant, Cement Plant and Smelting Plant: Huang et al., 2016; Traffic and Landfill Waste: Das et al., 2016; Coal: Yin et al., 2014; Sphalerites: Yin et al., 2016a, 2016b). The error bar stands for 1σ of δ^{202}Hg and Δ^{199}Hg of street dust in cities calculated from data in this study.

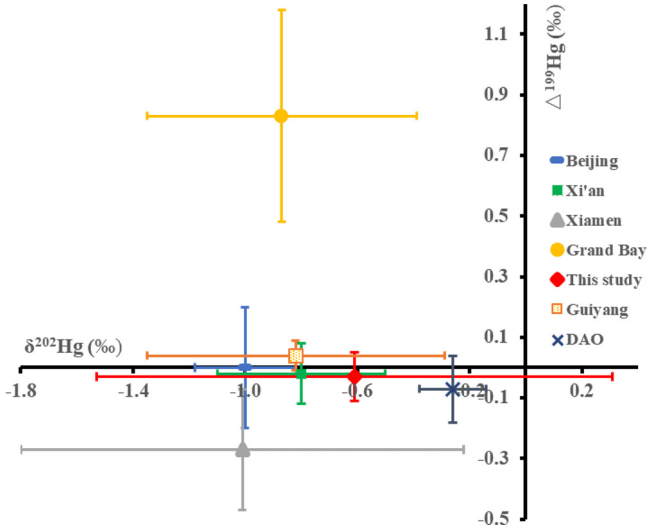

Fig. 3. δ^{202}Hg and Δ^{199}Hg values in TSP at four cities compared with that found in street dusts of this study. The error bar means 1σ of δ^{202}Hg and Δ^{199}Hg values calculated from data in this study and previous studies (Huang et al., 2020, 2018; Xu et al., 2017; Yu et al., 2016a, 2016b; Rolison et al., 2013).

Mississippi, United States (Rolison et al., 2013) which are shown in Fig. 3. Mean $\delta^{202}Hg_{dust}$ in this study was comparable to values observed in Asia and North America but it was lower than that in DAO of China. This difference suggested that δ^{202}Hg characteristic can distinguish different anthropogenic sources. The mean $\Delta^{199}Hg_{dust}$ in this study was comparable to the values observed in Beijing, Xi'an, DAO and Guiyang, but it was lower than values in the Grand Bay and higher than values observed in Xiamen, China. The Δ^{199}Hg signatures of street dust and TSP in urban areas of China were similar to those of anthropogenic emissions (−0.04‰) (Sun et al., 2016b) indicating that localized anthropogenic emissions shift the isotopic composition of TSP/dust toward lower Δ^{199}Hg values in urban areas.

Mercury isotope ratios (δ^{202}Hg, mean ± 1σ; Δ^{199}Hg, mean ± 1σ) of potential pollution sources were characterized from the literature for particulate materials from coal fired power plants (CFPP, δ^{202}Hg, −1.10 ± 1.20‰; Δ^{199}Hg, −0.10 ± 0.13‰), a cement plant (CP, δ^{202}Hg, −1.42 ± 0.36‰; Δ^{199}Hg, −0.05 ± 0.07‰), landfill waste (waste, δ^{202}Hg, −0.59 ± 0.13‰; Δ^{199}Hg, 0.02 ± 0.07‰), a Pb-Zn smelting plant (SP, δ^{202}Hg, −2.39 ± 0.72‰; Δ^{199}Hg, −0.16 ± 0.10‰), traffic exhaust (δ^{202}Hg, −1.54 ± 1.00‰; Δ^{199}Hg, 0.00 ± 0.19‰), coal (δ^{202}Hg, −0.97 ± 0.49‰; Δ^{199}Hg, −0.06 ± 0.14‰), sphalerite (δ^{202}Hg, −0.47 ± 0.47‰; Δ^{199}Hg, 0.02 ± 0.06‰) and organic soil (δ^{202}Hg, -0.79 ± 0.45‰; Δ^{199}Hg, -0.25 ± 0.14‰) (Huang et al., 2016; Das et al., 2016; Yin et al., 2014, 2016b; Sun et al., 2019a, 2019b). The Δ^{199}Hg signatures of urban street dust in this study were similar to those of anthropogenic emissions (−0.04‰) (Sun et al., 2016b). Considering that the background particle-bound Hg pool is characterized by significantly positive Δ^{199}Hg signatures (Fu et al., 2019), Hg in dust is believed to have originated mainly from local and regional emission sources rather than long-range transport because particle-bound Hg is removed faster than elemental Hg from the air (Schroeder and Munthe, 1998; Amos et al., 2012; Zhang et al., 2009). Considerable differences in isotopic compositions between dust samples collected in this study from 14 cities and the known sources in the published literature further indicate significant contributions to street dust by human activities. The average isotope composition (δ^{202}Hg vs. Δ^{199}Hg) in street dust in this study was distinct from that observed in organic soil (Sun et al., 2019a), which suggests the contribution of Hg in street dust from soil is very small. At present, the civilian use of coal, coal-fired power plants, cement plants, and traffic exhaust are the major contributors to particle-bound Hg detected in China (Men et al., 2018). The near-zero Δ^{199}Hg signature in dust is similar to the primary anthropogenic source and supports contributions dominated by anthropogenic sources (Fig. 2). Slightly positive MIF-199 signatures were observed in the KRL, EZ, SY, WH, HS, and GZ samples compared to those of the above-mentioned particulate sources, while the δ^{202}Hg variation ranges were relatively similar. Indeed, the isotopic composition obtained for each city can be considered a result of mixing from different Hg sources, each of which has its own isotope ratio, and can be affected by transport or transformation processes during both source and post-emission fractionation. Furthermore, the positive odd-MIF may have originated from photoreduction of Hg^{2+} in cloud droplets, as previously observed by Gratz et al. (2010) and Rolison et al. (2013). It is worth noting that the isotope compositions in HX were similar to those of particulate materials obtained from waste in a landfill site in Kolkata, India (Das et al., 2016), and were very different from the isotope composition of soil in Huaxi (δ^{202}Hg, −1.73 ± 0.08‰; Δ^{199}Hg, −0.21 ± 0.04‰; Yin et al., 2013), indicating that waste may be a possible contributor to Hg in dust. ZZ and HZ are cities with zinc smelting industries (Feng et al., 2006; Li et al., 2013), the similar isotopic compositions of dust in these two cities and that of sphalerite indicates that zinc smelting is also a major Hg

contributor. Similarly, Hg mine waste calcines (δ^{202}Hg, 0.08 ± 0.20‰; Δ^{199}Hg, ~0‰; Yin et al., 2013) were the major source of dust samples in XY and WS. When considering MDF in particular, some samples from ZZ, HZ, WH, HS, SHT, and XY displayed positive δ^{202}Hg values similar to those of coal combustion and sphalerite, as shown in Fig. 2.

The city of LS on the Tibetan Plateau is known to be mainly influenced by emissions from CFPP, CP, and traffic exhaust (Yuan et al., 2015). As discussed previously (Fig. 2), Hg emitted by these anthropogenic sources is characterized by negative δ^{202}Hg and near zero Δ^{199}Hg. However, more positive δ^{202}Hg and Δ^{199}Hg values than those from the known sources were obtained from the dust samples in LS, indicating that post-emission processes modified the initial isotope compositions. For example, it was previously reported that Hg in particles had similar Δ^{199}Hg values to, but more positive δ^{202}Hg values (0.51‰) than those of Hg in precipitation (Huang et al., 2016). Furthermore, positive odd-MIF Δ^{199}Hg values (i.e., from 0.38‰ to 0.76‰) have also been previously observed in precipitation Hg (Yuan et al., 2015). Previous studies have indicated that positive odd-MIF mainly occurs during photochemical reactions (Zheng and Hintelmann, 2010; Bergquist and Blum, 2007; Sun et al., 2016a; Zheng et al., 2019). The city of TS in northern China is famous for its steel industry. Dust samples collected in this city presented more positive δ^{202}Hg values and negative MIF-Δ^{199}Hg signatures than those of a smelting plant, that should be the result of a mixture of some pollution sources. As mentioned previously, SHT is famous for e-waste recycling, with an annual recycling capacity of 100,000 tonnes (Li et al., 2011). Positive δ^{202}Hg (0.36 ± 0.63‰) and near-zero Δ^{199}Hg values (0.10 ± 0.02‰) were observed in the dust samples collected from SHT. These isotopic signatures are believed to be attributable to e-waste recycling. However, it needs to be mentioned that the Hg isotope compositions of pollution sources were from limited data and regions. This will affect the accuracy of source determination and source contribution calculations.

3.4. Potential health risks of mercury in dust

Health risk assessment of the exposure of both adults and children to Hg in street dust was performed based on the model developed by the US Environmental Protection Agency (RAIS, 2018; USEPA, 2002, 1989; Zarandi et al., 2019a, 2019b). Three pathways of exposure were considered: ingestion of particles, inhalation of particles and vapor, and dermal absorption. According to the model formulas, exposure to Hg by ingestion is 100 and 10,000 times greater than by inhalation and dermal absorption, respectively. Therefore, ingestion is the major exposure pathways for dust expourse.

To evaluate the potential health risks for ingestion exposure to THg and MeHg in dust, the PDI value was calculated and compared to the relevant oral reference dose (RfD, $\mu g\,kg^{-1}\,d^{-1}$). The health risk is not a concern if PDI < RfD. The parameters used in this risk assessment are summarized in Table 2. Daily THg and MeHg intakes for adults and children were calculated using the concentrations determined in this study. To obtain an estimated "reasonable maximum exposure" (USEPA, 1989), a 95 % upper confidence limit for the mean Hg concentration was used. In addition, a mean value of 0.28 % was used to estimate MeHg from THg concentration for each city based on results of MeHg/THg ratio in WH (Sun et al., 2013), Xiamen (Liang et al., 2009), and GZ (Huang et al., 2012).

The health risk results of dust ingestion exposure to THg and MeHg based upon Monte Carlo simulations are shown in Fig. 4. The PDI of THg from dust consumption ranged from 2.86E–06 to 5.59E–02 $\mu g\,kg^{-1}\cdot d^{-1}$ with an average of 1.36E–03 $\mu g\,kg^{-1}\cdot d^{-1}$ for adults, and from 2.67E–05 to 5.22E–01 $\mu g\,kg^{-1}\cdot d^{-1}$ with an average of 1.27E–02 $\mu g\,kg^{-1}\cdot d^{-1}$ for children. The PDI values of THg were much higher for children than for adults, with 2.2 % of the children's PDI values exceeding the limit (0.16 $\mu g\,kg^{-1}\cdot d^{-1}$) set by OEHHA (2008), indicating that children are more susceptible to mercury pollution in street dust than adults (Hou et al., 2019; Yang et al., 2019). The PDI of MeHg from dust consumption had average values of 3.81E–06 and 3.56E–05 $\mu g\,kg^{-1}\cdot d^{-1}$ for adults and children, respectively, which are both lower than the limit (0.1 $\mu g\,kg^{-1}\cdot d^{-1}$) set by the USEPA (2010). However, 1.1 % of the children's PDI values of MeHg are above the half-limit, further confirming that children are exceptionally sensitive to MeHg contaminated dust due to their hand-to-mouth behavior (Hou et al., 2019; Yang et al., 2019).

The highest value of the calculated PDI of THg in China was 5.22E–01 $\mu g\,kg^{-1}bw\ d^{-1}$ for children in WS, which is a city with nearby historical mercury mining. The PDI of MeHg for this city was also higher than the RfD set by USEPA (0.1 $\mu g\,kg^{-1}bw\ d^{-1}$) (USEPA, 2010). Thus, children's exposure to mercury in dust is a major concern in areas with a history of, or current, mercury mining (e.g., WS and XY), and may also be a concern in cities with major coal-based industries and nonferrous metal smelting (e.g., SHT and ZZ). In comparison, the average PDIs of THg from rice consumption in China were 8.10E–03 and 1.27E–02 $\mu g\,kg^{-1}\cdot d^{-1}$ for adults and children, respectively (Zhao et al., 2019), which are comparable with those from street dust exposure. However, the average PDIs of MeHg from street dust exposure were far less than the exposure from rice consumption (Zhao et al., 2019; Zhang et al., 2010). The PDI of MeHg for children was 10 times greater than that of adults from street dust exposure, implying that children have a larger MeHg health risk. From the previous discussions we can conclude that health risks from ingestion of THg and MeHg in dust is of moderate concern for the majorities of Chinese cities and deserves more attention, especially for children.

However, some uncertainties still remain in our knowledge of potential health risks of mercury in dust of China. The exposure parameters control the accuracy of the risk assessment (Hou et al., 2019). There is no standard reference for exposure parameters in China. Many of the existing parameters are derived from western countries and are not sufficient to represent the exposure characteristics for Chinese residents (Juhasz et al., 2014; Cai et al., 2019). The parameter errors can cause large deviations, even when concentrations were measured accurately in health risk assessments.

4. Conclusions

In this study we reported distribution patterns of total Hg and Hg isotopic signatures of street dust from a number of Chinese cities. We found that the average total Hg concentration (0.43 $mg\,kg^{-1}$) in street dust was significantly higher than the background value (0.065 $mg\,kg^{-1}$) of Chinese soil and lower than the soil guideline value (1.0 $mg\,kg^{-1}$). Higher THg contents were observed in cities with nearby Hg and Zn smelting, e-waste recycling, and coal burning activities. Significant differences in mercury isotopic signals were observed between cities. Positive δ^{202}Hg and near-zero Δ^{199}Hg values (δ^{202}Hg, 0.36 ± 0.63 ‰; Δ^{199}Hg, 0.10 ± 0.02 ‰) were found in dust samples originating from e-waste sites for the first time. Results from the present study demonstrate the potential of using Hg isotopic signals to identify different pollution sources, although it should be noted that, when assigning source signatures, Hg isotope fractionation is possible during secondary fractionation processes. Further studies are needed to more confidently quantify the isotopic signatures of Hg sources. This study further suggests that the adverse effects of Hg on ecosystem and children's health require more attention in future studies. Crawling and finger-sucking habits increase the risk of Hg ingestion through the hand-mouth route, which has become the primary route for children to absorb Hg.

Declaration of Competing Interest

We declare that we have no financial and personal relationships with other people or organizations that can inappropriately influence our work, there is no professional or other personal interest of any

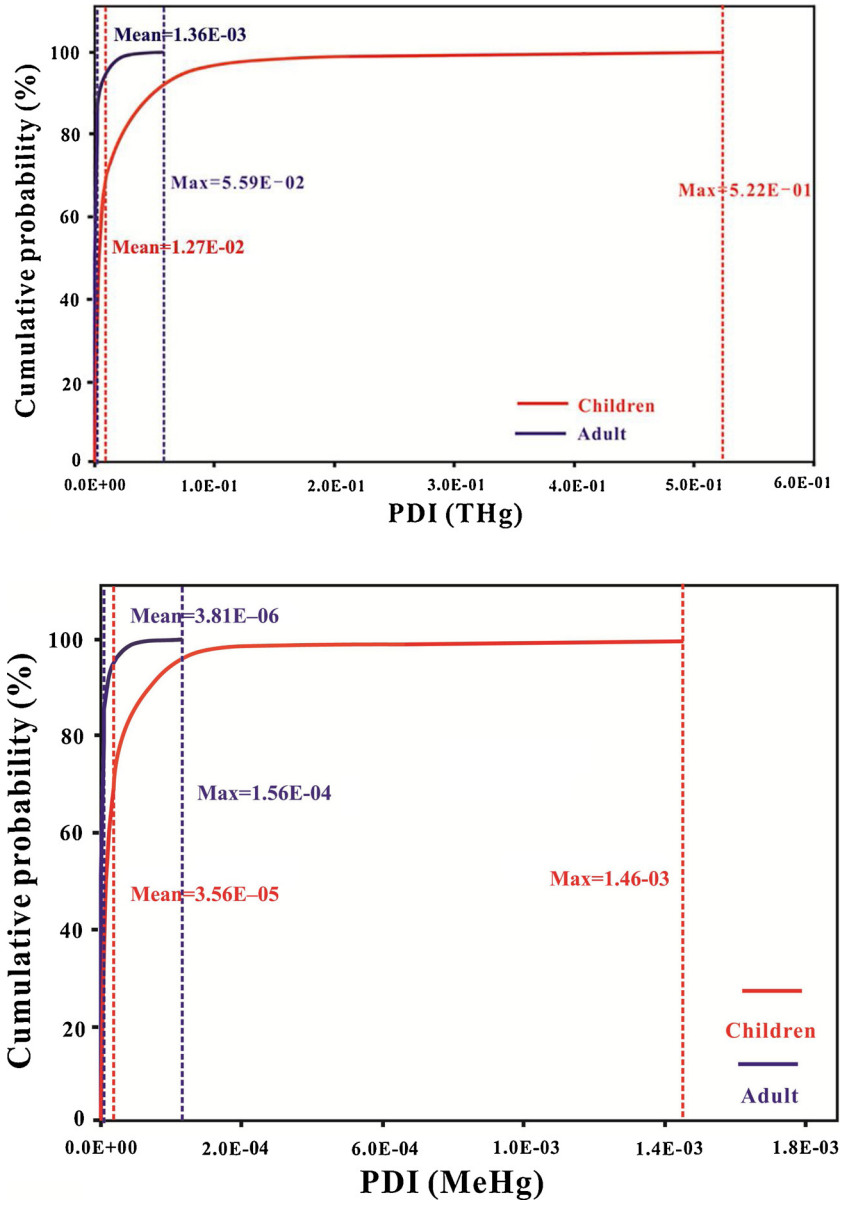

Fig. 4. Cumulative probability of PDI health risks posed by THg (upper panel) and MeHg (lower panel) in street dust.

nature or kind in any product, service and/or company that could be construed as influencing the position presented in, or the review of, the manuscript entitled.

CRediT authorship contribution statement

Guangyi Sun: Investigation, Data curation, Formal analysis, Writing - original draft. **Xinbin Feng:** Conceptualization, Resources, Supervision. **Chenmeng Yang:** Investigation. **Leiming Zhang:** Writing - review & editing. **Runsheng Yin:** Writing - review & editing. **Zhonggen Li:** Supervision. **Xiangyang Bi:** Investigation. **Yunjie Wu:** Investigation.

Acknowledgments

This study was funded by the Strategic Priority Research Program of the Chinese Academy of Sciences, Pan-Third Pole Environment Study for a Green Silk Road (Pan-TPE, XDA20040502), the National Science Foundation of China (grant nos. 41907286; 41773146), China Postdoctoral Science Foundation (2018M640939), the Bureau of Frontier Sciences and Education, the Chinese Academy of Sciences (grant no. QYZDJSSW-DQC005-02), and the K.C. Wong Education Foundation.

Appendix A. Supplementary data

Supplementary material related to this article can be found, in the online version, at doi:https://doi.org/10.1016/j.jhazmat.2020.122276.

References

Abuduwailil, J., Zhang, Z.Y., Jiang, F.Q., 2015. Evaluation of the pollution and human health risks posed by heavy metals in the atmospheric dust in Ebinur Basin in Northwest China. Environ. Sci. Pollut. Res. 22, 14018–14031.

Ambade, B., Litrupa, S., 2012. Evaluation of heavy metal contamination in road dustFallout of Bhilai city. Int. J. Adv. Eng. Res. 1, 81–83.

Amos, H.M., Jacob, D.J., Holmes, C.D., Fisher, J.A., Wang, Q., Yantosca, R.M., Corbitt, E.S., Galarneau, E., Rutter, A.P., Gustin, M.S., Steffen, A., Schauer, J.J., Graydon, J.A., St Louis, V.L., Talbot, R.W., Edgerton, E.S., Zhang, Y., Sunderland, E.M., 2012. Gasparticle partitioning of atmospheric Hg(II) and its effect on global mercury deposition. Atmos. Chem. Phys. 12 (1), 591–603.

Bergquist, B.A., Blum, J.D., 2007. Mass-dependent and -independent fractionation of Hg

isotopes by photoreduction in aquatic systems. Science 318, 417–420.
Blum, J.D., Bergquist, B.A., 2007. Reporting of variations in the natural isotopic composition of mercury. Anal. Bioanal. Chem. 388, 353–359.
Blum, J.D., Johnson, M.W., 2017. Recent developments in mercury stable isotope analysis. Rev. Mineral. Geochem. 82, 733–757.
Brown, A.D., Yalala, B., Cukrowska, E., Godoi, R.H.M., Vermaak, S.P., 2019. A scoping study of component-specific toxicity of mercury in urban road dusts from three international locations. Environ. Geochem. Health. https://doi.org/10.1007/s10653-019-00351-1.
Cai, L.M., Wang, Q.S., Luo, J., Chen, L.G., Zhu, R.L., Wang, S., Tang, C.H., 2019. Heavy metal contamination and health risk assessment for children near a large Cu-smelter in central China. Sci. Total Environ. 650, 725–733.
CEPA (Chinese Environmental Protection Administration), 1990. Elemental Background Values of Soils in China. Environmental Science Press of China, Beijing.
Chen, Z.X., Luan, W.L., 2011. Distribution characteristics and genetic analysis of heavy metals in near surface atmospheric dustfall in Tangshan. Geophys. Geochem. Explor. 35 (6), 833–836.
Dai, L.J., 2016. Study on the Law of Heavy Metals between Urban Top Soil and Street Dust. Master's Thesis. Guizhou Normal University.
Dai, J.R., Zhu, D.C., Pang, X.G., Wang, X., 2014. Geochemical characteristics and pollution sources identification of the near surface atmosphere dustfall in Jining city. China Environ. Sci. 34, 40–48 (in Chinese).
Dai, Y., Li, Z., Li, Y., Yang, Z., Chen, Y., 2015. Pollution characteristics of heavy metals instreet dust in main urban area of Chongqing. Environ. Chem. 34, 188–189 (in Chinese).
Das, R., Wang, X.F., Khezri, B., Webster, R.D., Sikdar, P.K., Datta, S., 2016. Mercury isotopes of atmospheric particle bound mercury for source apportionment study in urban Kolkata, India. Elementa 4, 1–12.
Dehghani, M., Jarahzadeh, S., Hadie, M., Mansouri, N., Rashidi, Y., Yousefi, M., 2018. The data on the dispersion modeling of traffic-related PM10 and CO emissions using CALINE3: a case study in Tehran, Iran. Data Brief 19, 2284–2290.
Dehghani, M.H., Hopke, P., Asghari, F.B., Mohammadi, A.A., Yousefi, M., 2019. The effect of the decreasing level of Urmia Lake on particulate matter trends and attributed health effects in Tabriz, Iran. Microchem. J. 19, 104434.
Demers, J.D., Sherman, L.S., Blum, J.D., Marsik, F.J., Dvonch, J.T., 2015. Coupling atmospheric mercury isotope ratios and meteorology to identify sources of mercury impacting a coastal urbanindustrial region near Pensacola, Florida, USA. Glob. Biogeochem. Cycles 29 (10), 1689–1705.
Deng, C.Z., Sun, G.Y., Yang, W., et al., 2012. Analysis of the deposition flux and source of heavy metal elements in atmospheric dustfall in Gannan county, Heilongjiang Province. Earth Environ. 40, 342–348 (in Chinese).
Du, P.X., Tian, H., Han, Y.M., 2004. Concept, research content and method of urban dust. Geol. Shaanxi 22, 73–79 (in Chinese).
Duan, Z.Y., Su, H.T., Wang, F.Y., Zhang, L., Wang, S.X., Yu, B., 2016. Mercury distribution characteristics and atmospheric mercury emission factors of typical waste incineration plants in Chongqing. Environ. Sci. (Huanjingkexue) 37 (2), 459–465 (in Chinese).
Estrade, N., Carignan, J., Sonke, J.E., Donard, O.F.X., 2010. Measuring Hg isotopes in bio-geo-Environmental reference materials. Geostand. Geoanalytical Res. 34, 79–93.
Fang, F.M., Zhang, Z.M., Chen, W.J., Yang, D., 2009. Spatial and particle size distribution of mercury and arsenic on surface dust in spring in the Wuhu urban district. Acta Scientiae Circumstantiae 29 (9), 1871–1877.
Feng, X.B., Li, G.H., Qiu, G.L., 2006. A preliminary study on mercury contamination to the environment from artisanal zinc smelting using indigenous methods in Hezhang County, Guizhou, China: part 2. Mercury contaminations to soil and crop. Sci. Total Environ. 368, 47–55.
Fu, X.W., Feng, X.B., Sommar, J., et al., 2012. A review of studies on atmospheric mercury in China. Sci. Total Environ. 421/422, 73–81.
Fu, X.W., Zhang, H., Feng, X.B., Tan, Q.Y., Ming, L.L., Liu, C., 2019. Domestic and transboundary sources of atmospheric particulate bound mercury in remote areas of China: evidence from mercury isotopes. Environ. Sci. Technol. 53, 1947–1957.
Gratz, L.E., Keeler, G.J., Blum, J.D., Sherman, L.S., 2010. Isotopic composition and fractionation of mercury in Great Lakes precipitation and ambient air. Environ. Sci. Technol. 44, 7764–7770.
Gu, J.W., 2014. Progress in research on the contamination of heavy metals in urban street dust in China. Earth Environ. 42, 695–701 (in Chinese).
Han, X., Lu, X., Qing, G., Wu, Y., 2017. Health risks and contamination levels of heavy metals in dusts from parks and squares of an Industrial city in semi-arid area of China. Int. J. Environ. Res. Public Health 14, 886. https://doi.org/10.3390/ijerph14080886.
Hou, J.W., Gao, B.J., Lang, B., Pan, G.J., Zhou, L.W., 2015. Spatial distribution pattern of mercury in surface dust and its relationship with magnetic particles in Shanghai Wujing area. Environ. Sci. Technol. 38 (7), 48–52 (in chinese).
Hou, S.G., Zheng, N., Tang, L., et al., 2019. Pollution characteristics, sources, and health risk assessment of human exposure to Cu, Zn, Cd and Pb pollution in urban street dust across China between 2009 and 2018. Environ. Int. 128, 430–437.
Huang, M.J., Wang, W., Leung, H., Chan, C.Y., Liu, W.K., Wong, M.H., Cheung, K.C., 2012. Mercury levels in road dust and household TSP/PM2.5 related to concentrations in hair in Guangzhou, China. Ecotoxicol. Environ. Saf. 81, 27–35.
Huang, Q., Liu, Y.L., Chen, J.B., Feng, X.B., Huang, W.L., Yuan, S.L., Cai, H.M., Fu, X.W., 2015. An improved dual-stage protocol to pre-concentrate mercury from airborne particles for precise isotopic measurement. J. Anal. At. Spectrom. 30 (4), 957–966.
Huang, Q., Chen, J.B., Huang, W.L., et al., 2016. Isotope composition for source identification of mercury in atmospheric fine particles. Atmos. Chem. Phys. 16, 11773–11786.
Huang, S., Sun, L., Zhou, T., Yuan, D., Du, B., Sun, X., 2018. Natural stable isotopic compositions of mercury in aerosols and wet precipitations around a coal-fired power plant in Xiamen, southeast China. Atmos. Environ. 173, 72–80.
Huang, Q., Chen, J.B., Huang, W.L., et al., 2019. Diel variation in mercury stable isotope ratios records photoreduction of PM2.5-bound mercury. Atmos. Chem. Phys. 19, 315–325.
Huang, Q., Reinfelder, J.R., Fu, P.Q., Huang, W.L., 2020. Variation in the mercury concentration and stable isotope composition of atmospheric total suspended particles in Beijing, China. J. Hazard. Mater. 383, 121131.
Juhasz, A.L., Paul, H., Carina, H., John, B., Euan, S., 2014. Validation of the predictive capabilities of the Sbrc-G in vitro assay for estimating arsenic relative bioavailability in contaminated soils. Environ. Sci. Technol. 48, 12962–12969.
Lai, M.S., Yang, Z.F., Wang, H.C., et al., 2008. Effects of atmospheric fallouts on heavy metal elements accumulation in soils in farmland areas in the Taiyuan basin, Shanxi, China and sources of fallouts. Geol. Bull. China 27, 240–245 (in Chinese).
Li, D.Y., Liao, Y.L., 2018. Spatial characteristics of heavy metals in street dust of coal railway transportation hubs: a case study in Yuanping, China. Int. J. Environ. Res. Public Health 15, 2662.
Li, B., Du, H.Z., Ding, H.J., Shi, M.Y., 2011. E-waste recycling and related social issues in China. Energy Procedia 5, 2527–2531.
Li, Z.G., Feng, X.B., Li, G.H., Bi, X.Y., Zhu, J.M., Qin, H.B., et al., 2013. Distributions, sources and pollution status of 17 trace metal/metalloids in the street dust of a heavily industrialized city of central China. Environ. Pollut. 182, 408–416.
Li, H., Qian, X., Wei, H., et al., 2014. Magnetic properties as proxies for the evaluation of heavy metal contamination in urban street dusts of Nanjing, Southeast China. Geophys. J. Int. 199, 1354–1366.
Li, C.H., Liang, H.D., Chen, Y., et al., 2017. Distribution of mercury content in dusts of coal base, Wuda, China. China Environ. Sci. 37, 2203–2210 (in Chinese).
Li, F., Huang, J.H., Zeng, G.M., Huang, X.L., et al., 2015a. Spatial distribution and health risk assessment of toxic metals associated with receptor population density in stret dust: a case study of Xiandao District, Changsha, Middle China. Environ. Sci. Pollut. Res. 22, 6732–6742.
Li, H., Wang, M.S., Wang, M.Y., et al., 2015b. Health risk assessment of heavy metals pollution of dust in China. Resour. Dev. Market 31, 803–807 (in Chinese).
Liang, Y., Yuan, D.X., Lu, M., et al., 2009. Distribution characteristics of total mercury and methylmercury n the topsoil and dust of Xiamen, China. J. Environ. Sci. 21 (10), 1400–1408.
Lin, Y.Z., 2017. The Geochemical Characteristics and Environmental Evaluation of Quality in Mercury Mine Area of Guizhou Wanshan. Master's Thesis. Chengdu Univerisity of Technology.
Lin, H.Y., Zhu, X.T., Feng, Q.G., Guo, J.D., Sun, X.L., Liang, Y., 2019. Pollution, sources, and bonding mechanism of mercury in street dust of a subtropical city, southern China. Hum. Ecol. Risk Assess. 25, 393–409.
Liu, C., Liao, Q., Huang, S.S., Jin, Y., Zhu, B.W., Huang, M., 2009. Studies on trace elements geochemistry of atmospheric dust and related issues in urban geological survey in Jiangsu. J. Geol. 33, 138–149 (in Chinese).
Lu, X., Zhao, J.T., Liang, X.J., et al., 2019. The application and potential artifacts of Zeeman cold vapor atomic absorption spectrometry in mercury stable isotope analysis. Environ. Sci. Technol. Lett. 6 (3), 165–170.
Lu, X.W., Li, L.Y., Wang, L.J., Lei, K., et al., 2009. Contamination assessment of mercury and arsenic in roadway dust from Baoji, China. Atmos. Environ. 43, 2489–2496.
Ma, Z.W., Chen, K., Li, Z.Y., Bi, J., Huang, L., 2016. Heavy metals in soils and road dusts in the mining areas of Western Suzhou, China: a preliminary identification of contaminated sites. J. Soils Sediments 16, 204–214.
Mao, G.C., Gu, Y.L., Hu, D.B., et al., 2016. Analysis of heavy metal content situation in the environment and students' hair samples in Ninbo urban area. J. Saf. Environ. 16, 323–328.
Marcazzan, G., Vaccaro, S., Valli, G., et al., 2001. Characterisation of PM10 and PM2.5 particulate matter in the ambient air of Milan (Italy). Atmos. Environ. 35 (27), 4639–4650.
Marx, S.K., Kamber, B.S., Mcgowan, H.A., 2008. Scavenging of atmospheric trace metal pollutants by mineral dusts: interregional transport of Australian trace metal pollution to New Zealand. Atmos. Environ. 42 (10), 2460–2478.
Men, C., Liu, R.M., Xu, F., Wang, Q.R., Guo, L.J., Shen, Z.Y., 2018. Pollution characteristics, risk assessment, and source apportionment of heavy metals in road dust in Beijing, China. Sci. Total Environ. 612, 138–147.
Nabizadeh, R., Yousefi, M., Azimi, F., 2018. Study of particle number size distributions at Azadi terminal in Tehran, comparing high-traffic and no traffic area. MethodsX 5, 1549–1555.
Nazarpour, A., Ghanavati, N., Watts, M.J., 2017. Spatial distribution and human health risk assessment of mercury in street dust resulting from various land-use in Ahvaz, Iran. Environ. Geochem. Health. https://doi.org/10.1007/s10653-017-0016-5.
OEHHA. Revised Air Toxics Hot Spots Program Technical Support Document for the Derivation of Non-cancer Reference Exposure Levels and RELs for Six Chemicals, 2008.California Environmental Protection Agency, Office of Environmental Health HazardAssessment, US.
Ordóñez, A., Álvarez, R., De Miguel, E., Charlesworth, S., 2015. Spatial and temporal variations of trace element distribution in soils and street dust of an industrial town in NW Spain: 15 years of study. Sci. Total Environ. 524–525, 93–103.
Qasemi, M., Shams, M., Sajjadi, S.A., Farhang, M., Erfanpoor, S., Yousefi, M., Zarei, A., Afsharnia, M., 2019. Cadmium in groundwater consumed in the rural areas of Gonabad and Bajestan, Iran: occurrence and health risk assessment. Biol. Trace Element Res. 192, 106–115 Volume.
RAIS, 2018. The Risk Assessment Information System, Toxicity Profiles, Condensed Toxicity Summary for Mercury. https://rais.ornl.gov/tox/profiles/mercury_c_V1.htmlSchroeder.
Rolison, J.M., Landing, W.M., Luke, W., Cohen, M., Salters, V.J.M., 2013. Isotopic composition of species-specific atmospheric Hg in a coastal environment. Chem. Geol.

336, 37–49.
Rostami, R., Zarei, A., Saranjam, B., Ghaffari, H.R., Hazrati, S., Poureshg, Y., Fazlzadeh, M., 2019. Exposure and risk assessment of PAHs in indoor air of waterpipe cafés in Ardebil, Iran. Build. Environ. 155, 47–57.
Schroeder, W.H., Munthe, J., 1998. Atmospheric mercury – an overview. Atmos. Environ. 32, 809–822.
Shao, Q.N., Li, B., Qiu, J.C., Zhang, X., 2019. Analysis of heavy metal environmental characteristics of atmospheric dust in Lanshan area. Environ. Protect. Circular Econ. 1, 61–71 (in Chinese).
Streets, D.G., Hao, J., Wu, Y., et al., 2005. Anthropogenic mercury emissions in China. Atmos. Environ. 39, 7789–7806.
Sun, G., Sommar, J., Feng, X., Lin, C.-J., Ge, M., Wang, W., Yin, R., Fu, X., Shang, L., 2016a. Mass-dependent and -independent fractionation of mercury isotope during gas-phase oxidation of elemental mercury vapor by atomic Cl and Br. Environ. Sci. Technol. 50 (17), 9232–9241.
Sun, R.Y., Streets, D.G., Horowitz, H.M., Amos, H.M., Liu, G.J., Perrot, V., Toutain, J.P., Hintelmann, H., Sunderland, E.M., Sonke, J.E., 2016b. Historical (1850 – 2010) mercury stable isotope inventory from anthropogenic sources to the atmosphere. Elementa 4 (91), 000091.
Sun, R.Y., Jiskra, M., Amos, H.M., Zhang, Y.X., Sunderland, E.M., Sonke, J.E., 2019a. Modelling the mercury stale isotope distribution of earth surface reservoirs: implications for global Hg cycling. Geochimica et Cosmochimica Acta 246, 156–173.
Sun, J., Shen, Z., Zhang, L., Lei, Y., Gong, X., Zhang, Q., Zhang, T., Xu, H., Cui, S., Wang, Q., Cao, J., Tao, J., Zhang, N., Zhang, R., 2019b. Chemical source profiles of urban fugitive dust PM2.5 samples from 21 cities across China. Sci. Total Environ. 649, 1045–1053.
Tan, X.L., Shi, Z.M., Zhang, C.J., Ni, S.J., Luo, G., 2008. Studies on elemental geochemistry zoning in air dust near the ground of Chengdu city. Guangdong Weiliang Yuansu Kexue 15, 24–29 (in Chinese).
Tang, Z.W., Chai, M., Cheng, J.L., Jin, J., Yang, Y., Nie, Z.Q., Huang, Q.F., Li, Y.H., 2017. Contamination and health risks of heavy metals in street dust from a coal-mining city in eastern China. Ecotoxicol. Environ. Saf. 138, 83–91.
Tian, H., Zhou, G.L., Zheng, Q.B., et al., 2006. Study on dust transport and its relationship with the dust diameter in Hangzhou. J. Sichuan Agric. Univ. 24, 422–425 (in Chinese).
USEPA. Superfund Public Health Evaluation Manual, 1986. EPA/540/1-86 /060. Environmental Protection Agency, Washington, DC, pp. 1-52.
USEPA, 1989. Risk Assessment Guidance for Superfund, Vol.I: Human Health Evaluation Manual. office of emergency and remedial response, Washington, DC, pp. 43–57.
USEPA, 2001. Risk Assessment Guidance for Superfund: Volume III-Part A, Process for Conducting Probabilistic Risk Assessment. Washington, D.C. EPA 540-R-02-002.
US EPA, 2002. Supplemental Guidance for Developing Soil Screening Levels for Superfund Sites. United States Environmental Protection Agency.
USEPA, 2011. Supplemental Guidance for developing soil screening levels for Superfund sites. Office of Solid Waste and Emergency Response (OSWER).
USEPA. Guidance for Implementing the January 2010 Methylmercury WaterQuality Criterion, 2010. U.S. Environmental Protection Agency, Washington, DC.
Wang, X.Q., the CGB Sampling Team, 2015. China geochemical baselines: sampling methodology. J. Geochem. Explor. 148, 25–39.
Wang, J.H., Li, S.W., Cui, X.Y., Li, H.M., Qian, X., Wang, C., Sun, Y.X., 2016. Bioaccessibility, sources and health risk assessment of trace metals in urban park dust in Nanjing, Southeast China. Ecotoxicol. Environ. Saf. 128, 161–170.
Wei, B.G., Yang, L.S., 2010. A review of heavy metal contaminations in urban soils, urban road dusts and agricultural soils from China. Micochem. J. 94, 99–107.
Wiederhold, J.G., 2010. Metal stable isotope signatures as tracers in environmental geochemistry. Environ. Sci. Technol. 49, 2606–2624.
Wright, L.P., Zhang, L., Cheng, I., Aherne, J., Wentworth, G.R., 2018. Impacts and effects indicators of atmospheric deposition of major pollutants to various ecosystems – a review. Aerosol Air Qual. Res. 18, 1953–1992.
Wu, Q.R., Li, G.L., Wang, S.X., Liu, K.Y., Hao, J.M., 2018. Mitigation options of atmospheric Hg emissions in China. Environ. Sci. Technol. 52, 12368–12375.
Xu, H.M., Sonke, J.E., Guinot, B., et al., 2017. Seasonal and annual variations in atmospheric Hg and Pb isotopes in Xi'an, China. Environ. Sci. Technol. 51, 3759–3766.
Yang, Z.P., 2008. Eco-geochemical Characteristics and Sources Identification of Heavy Metal Contamination in Changchun City, China. PhD's thesis. Jilin University.
Yang, S.Y., Zhao, J., Chang, S.X., Collins, C., et al., 2019. Status assessment and probabilistic health risk modeling of metals accumulation in agriculture soils across china: a synthesis. Environ. Int. 128, 165–174.
Yao, Z., Zhang, Y.F., Dong, J.L., Tian, X.Y., 2017a. Geochemical characteristics of dustfall in the eastern part of Qinghai province, China. Min. Magazine 26, 170–172 (in Chinese).
Yao, Y.R., Fang, F.M., Wu, J.Y., Zhu, Z., Lin, Y.S., Zhang, D.L., Zhu, H.P., 2017b. Concentrations and pollution assessment of mercury in surfaces dust at urban strets and elementary school campuses of Huainan city. Aca Scientiac Circumstantiae 37 (3), 844–852.
Yin, R.S., Feng, X.B., Wang, J.X., et al., 2013. Mercury isotope variations between bioavailable mercury fractions and total mercury in mercury contaminated soil in Wanshan mercury mine, SW China. Chem. Geol. 336, 80–86.
Yin, R.S., Feng, X.B., Chen, J.B., 2014. Mercury stable isotopic compositions in coals from major coal producing fields in China and their geochemical and environmental implications. Environ. Sci. Technol. 48 (10), 5565–5574.
Yin, R.S., Krabbenhoft, D.P., Bergquist, B.A., et al., 2016a. Effects of mercury and thallium concentrations on high precision determination of mercury isotopic composition by Neptune plus multiple collector inductively coupled plasma mass spectrometry. J. Anal. At. Spectrom. 31 (10), 2060–2068.
Yin, R.S., Feng, X.B., Hurley, J.P., Krabbenhoft, D.P., Lepak, R.F., Hu, R.Z., Zhang, Q., Li, Z.G., Bi, X.W., 2016b. Mercury isotopes as proxies to identify sources and environmental impacts of mercury in Sphalerites. Sci. Rep. 6, 18686.
Yu, Y., Li, Y.X., Li, B., et al., 2016a. Metal enrichment and lead isotope analysis for source apportionment in the urban dust and rural surface soil. Environ. Pollut. 216, 764–772.
Yu, B., Fu, X., Yin, R., Zhang, H., Wang, X., Lin, C.-J., Wu, C., Zhang, Y., He, N., Fu, P., Wang, Z., Shang, L., Sommar, J., Sonke, J.E., Maurice, L., Guinot, B., Feng, X., 2016b. Isotopic composition of atmospheric mercury in China: new evidence for sources and transformation processes in air and in vegetation. Environ. Sci. Technol. 50 (17), 9262–9269.
Yuan, S., Zhang, Y., Chen, J., Kang, S., Zhang, J., Feng, X., Cai, H., Wang, Z., Wang, Z., Huang, Q., 2015. Large variation of mercury isotope composition during a single precipitation event at Lhasa city, Tibetan Plateau, China. Procedia Earth Planet. Sci. 13, 282–286.
Yunesian, M., Rostami, R., Zarei, A., Fazlzadeh, M., Janjani, H., 2019. Exposure to high levels of PM2.5 and PM10 in the metropolis of Tehran and the associated health risks during 2016–2017. Microchem. J. 150, 104174.
Zarandi, S.M., Shahsavani, A., Khodagholi, F., Fakhri, Y., 2019a. Concentration, sources and human health risk of heavy metals and polycyclic aromatic hydrocarbons bound PM2.5 ambient air, Tehran, Iran. Environ. Geochem. Health 41 (3), 1473–1487.
Zarandi, S.M., Shahsavani, A., Khodagholi, F., Fakhri, Y., 2019b. Co-exposure to ambient PM2.5 plus gaseous pollutants increases amyloid β1–42 accumulation in the hippocampus of male and female rats. J. Toxin Rev. https://doi.org/10.1080/15569543.2019.1611604.
Zhang, L., Wright, L.P., Blanchard, P., 2009. A review of current knowledge concerning dry deposition of atmospheric mercury. Atmos. Environ. 43, 5853–5864.
Zhang, H., Feng, X., Larssen, T., et al., 2010. In inland China, rice, rather than fish, is the major pathway for methylmercury exposure. Environ. Health Perspect. 118 (9), 1183–1188.
Zhang, C.R., Wu, Z.L., Yao, C.H., Gao, Z.J., 2014a. Health risk assessment of heavy metals in atmospheric dust of Qingdao City. Environ. Sci. 35, 2736–2741 (in Chinese).
Zhang, D.Y., Lee, D.J., Pan, X.L., 2014b. Potentially harmful metals and metalloids in urban street dusts of Urumqi city: comparison with Taipei city. J. Taiwan Inst. Chem. Eng. 45, 2447–2450.
Zhang, W.L., Du, Y., Zhai, M.M., Shang, Q., 2014c. Cadmium exposure and its health effects: a 19-year follow-up study of a polluted area in China. Sci. Total Environ. 470-471, 224–228.
Zhang, D.Y., Pan, X.L., Lee, D.J., 2014d. Potentially harmful metals and metalloids in the urban street dusts of Taipei City. J. Taiwan Inst. Chem. Eng. 45, 1727–1732.
Zhang, X.Y., Wang, D.Q., Cai, Y.W., et al., 2015. Concentration and health risk assessment of mercury in indoor dust in Shanghai. Urban Environ. Urban Ecol. 28, 29–32 (in Chinese).
Zhao, H., Yan, H., Zhang, L., et al., 2019. Mercury contents in rice and potential health risks across China. Environ. Int. 126, 406–412.
Zheng, W., Hintelmann, H., 2010. Isotope fractionation of mercury during its photochemical reduction by low-molecular-weight organic compounds. J. Phys. Chem. A 114, 4246–4253.
Zheng, W., Demers, J.D., Lu, X., Bergquist, B.A., Anbar, A.D., Blum, J.D., Gu, B.H., 2019. Mercury stable isotope fractionation during abiotic dark oxidation in the presence of thiols and natural organic matter. Environ. Sci. Technol. 53, 1853–1862.